Microencapsulation of Isocyanates for Self-Healing Polymers

Jinglei Yang,[†] Michael W. Keller,[†] Jeffery S. Moore,[†,‡,§] Scott R. White,[†,||] and Nancy R. Sottos*[,†,‡]

Beckman Institute, Department of Materials Science and Engineering, Department of Chemistry, and Department of Aerospace Engineering, University of Illinois at Urbana−Champaign, Urbana, Illinois 61801

Received July 29, 2008; Revised Manuscript Received October 29, 2008

ABSTRACT: Microcapsules containing reactive diisocyanate for use in self-healing polymers are successfully fabricated via interfacial polymerization of polyurethane (PU). Isocyanates are potential catalyst-free healing agents for use in humid or wet environments. The preparation of PU prepolymer and microencapsulation of isophorone diisocyanate (IPDI) healing agent are presented. Smooth spherical microcapsules of 40−400 μm in diameter are produced by controlling agitation rate (500−1500 rpm) according to a power law relation ($n = -2.24$). The PU shell wall thickness varies linearly with capsule diameter, such that the capsules wall thickness to diameter ratio is constant (∼0.05). High yields (∼70%) of a free-flowing powder of IPDI/PU capsules are produced with a liquid core content of 70 wt % as determined by TGA analysis. The microcapsules are stable with only ∼10 wt % loss of IPDI detected after 6 months storage under ambient conditions. Direct mechanical compression testing of microcapsules reveals a brittle fracture mode and normalized shell wall strength that varies with capsule diameter in a power law fashion ($n = -0.77$).

1. Introduction

Self-healing materials[1−5] represent a new paradigm for active and responsive materials. In a first generation self-healing system,[6] a microencapsulated liquid healing agent, *endo*-dicyclopentadiene (*endo*-DCPD), and solid phase Grubbs' catalyst are embedded in an epoxy matrix. When a microcrack propagates through the material, it ruptures the microcapsules and releases the healing agent into the damaged region, where it undergoes a polymerization upon mixing with the catalyst phase. This microcapsule motif has been extended to other matrix materials and healing chemistries.[7−18] Other self-healing approaches have also been demonstrated including incorporating hollow glass fibers in fiber-reinforced composites[19−23] and embedded vascular networks.[24−26] Wudl and co-workers[27−30] have also introduced thermally remendable polymers for self-healing purposes.

Self-healing polymers are a high value target for advanced coatings to prevent corrosion via formation of new material[31−34] or release of inhibitor[33,35,36] in the damaged area. The repaired maintenance costs attributed to corrosion are significant.[37] A microcapsule-based self-healing coating was recently demonstrated based on a PDMS healing chemistry[38] that showed excellent corrosion prevention following surface damage.[31] However, more robust healing chemistries are required to enable self-healing in harsh environments (e.g., underwater).

In this paper we investigate the encapsulation of a liquid-phase diisocyanate monomer healing agent via interfacial polymerization in a stabilized aqueous emulsion. Previous work on the encapsulation of isocyanates has been limited to the solid state or blocked form.[39−41] The encapsulated material in this study is isophorone diisocyanate (IPDI), a monomeric aliphatic diisocyanate widely used in abrasion and UV-resistant polyurethane (PU) coatings.[42] Diisocyanates are reactive with water, introducing the possibility of one-part, catalyst-free self-healing system that is functional in an aqueous or moisture-laden environment.

* Corresponding author: e-mail n-sottos@uiuc.edu.
[†] Beckman Institute.
[‡] Department of Materials Science and Engineering.
[§] Department of Chemistry.
[||] Department of Aerospace Engineering.

2. Experimental Section

2.1. Preparation of Prepolymer and Microcapsules. *Preparation of Prepolymer.* Toluene diisocyanate (TDI) prepolymer is prepared as a constituent material for the microcapsule shell wall. A representative synthesis route is shown in the Supporting Information (Scheme 1). All chemicals used in this study were purchased at reagent grade and used without further purification unless otherwise specified. Toluene 2,4-diisocyanate (TDI, 21.85 g, Sigma-Aldrich) was dissolved into cyclohexanone (141.65 g, Sigma-Aldrich) in a 250 mL round-bottom flask. The mixture was then suspended in an 80 °C oil bath and agitated using a magnetic stirrer. 1,4-Butanediol (BD, 4.12 g, Sigma-Aldrich) was slowly added. The flask was purged with N_2 and allowed to react for 24 h. The mixture was then distilled at 100 °C under 15 Torr for 4−5 h. Cyclohexanone, water, and excess TDI were removed into the receiving trap, leaving a yellowish, viscous prepolymer in the flask. The molecular weight of the synthesized prepolymer was 1270 for number-average ($\bar{M}_n$) and 1690 for weight-average ($\bar{M}_w$) by gel permeation chromatography.[31] Thus, the polydispersity index (PDI) of the prepolymer was 1.33.

Synthesis of Microcapsules. At room temperature, 30 mL of deionized water and gum arabic (4.5 g, Sigma Aldrich) surfactant[43] were mixed in a 100 mL beaker. The beaker was suspended in a temperature-controlled water bath on a programmable hot plate with an external temperature probe. The solution was agitated with a digital mixer (Eurostar, IKA Labortechnik), driving a three-bladed propeller for 3 h before beginning encapsulation.

To prepare the microencapsulation solution, the prepolymer (2.9 g) was dissolved into chlorobenzene (ClB, 4 g, Sigma Aldrich) at 68 °C. Once the prepolymer was completely dissolved, IPDI (9.5 g, Bayer MaterialScience) was added and mixed well. The mixture was then slowly poured into the gum arabic solution. The water bath was heated to 70 °C at a rate of 7 °C/min. At 50 °C, 1,4-butanediol (3.1 g) as a chain extender was slowly added to the emulsion. After 45 min of agitation the mixer and hot plate were switched off. Polyurethane shell was formed at the interface between the aqueous phase and oil phase, as schematically shown in Figure 1. Once cooled to ambient temperature, the suspension of microcapsules was rinsed with deionized water and vacuum filtered. Microcapsules were air-dried for 48 h before further analysis. The average yield of microcapsules was about 70 wt % for agitation rates ranging from 500 to 1500 rpm.

10.1021/ma801718v CCC: $40.75
Published on Web 11/25/2008

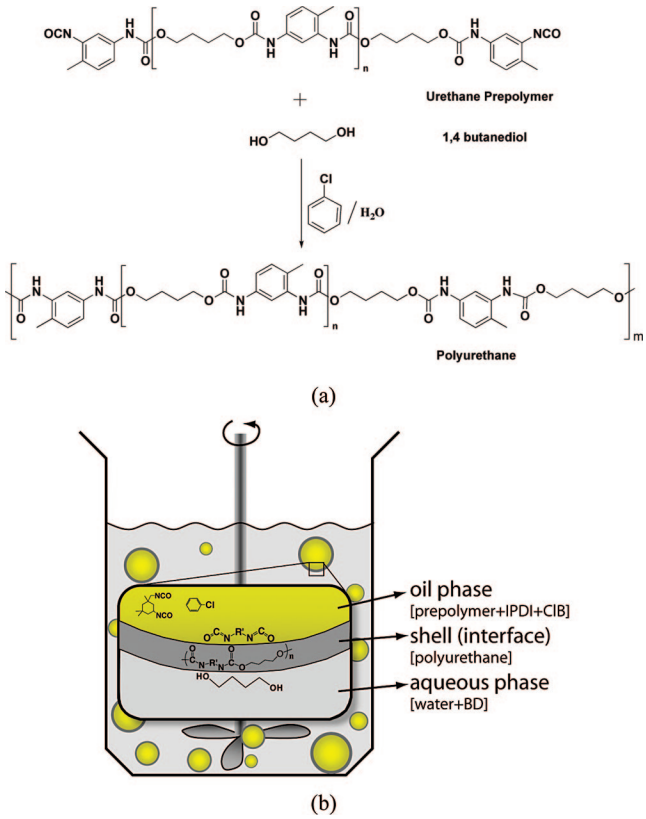

Figure 1. (a) Reaction scheme for microencapsulation using interfacial polymerization. (b) Schematic diagram of capsule shell wall formation under mechanical agitation.

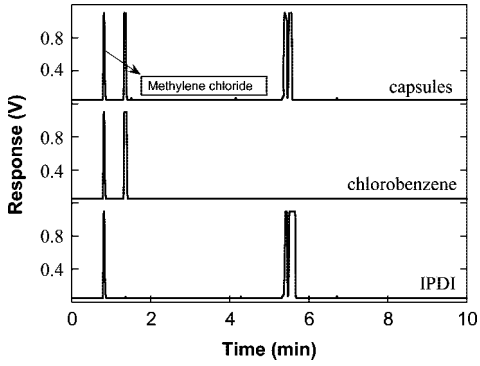

Figure 2. Gas chromatography traces of microcapsule contents along with pure ClB and IPDI controls.

2.2. Characterization of Prepolymer and Microcapsules. *Titration of NCO Content in Prepolymer.* The synthesized prepolymer (0.15 g) and dry toluene (25 mL) were added in a 250 mL Erlenmeyer flask with a stopper. The prepolymer was dissolved with help of a mechanical agitator. Di-*n*-butylamine solution (25 mL, 0.1 N) was added using a pipet. After swirling for 15 min, isopropyl alcohol (100 mL) and bromphenol blue indicator solution (4−6 drops) were added. Two titrations were performed with hydrochloride acid (0.1 N) to a yellow end point. Two blank titrations were run including all reagents above but omitting the prepolymer. The NCO content is calculated as follows:

$$\text{NCO}, \% = \frac{[(B - V) \times N \times 0.0420]}{W} \times 100 \qquad (1)$$

where B and V (both in mL) are the volumes of HCl for titration of the blank and the prepolymer, respectively, N normality of HCl, and W grams of prepolymer.

Microcapsule Size. Microcapsule size was analyzed using a Leica optical microscope and Micropublisher CCD camera and image analysis software (ImageJ V1.3.8). Mean diameter and standard deviation were determined from data sets of at least 250 measurements.

Morphology of Microcapsules. Surface morphology and capsule shell thickness were examined by scanning electron microscopy (XL30 ESEM-FEG, Philips). Microcapsules were mounted on a conductive stage and ruptured with a razor blade to facilitate membrane thickness measurement. Samples were sputtered with a thin layer (∼10 nm) of gold−palladium to reduce charging.

Gas Chromatography (GC). A Hewlett-Packard 5890 Series II gas chromatograph (GMI, Inc.) with a 530 μm internal diameter capillary column and flame ionization detector was used to qualitatively determine the core materials in microcapsules. The temperature was linearly ramped at a heating rate of 20 °C/min. GC samples were prepared by crushing microcapsules in a vial and adding methylene chloride. The mixture was then filtered and the liquid collected for testing. Two control tests of pure chlorobenzene and IPDI were performed for comparison.

Thermogravimetric Analysis. Thermogravimetric analysis (Mettler-Toledo TGA-4400) was used to investigate the thermal stability of the prepared capsules. Small amounts of microcapsules (10−20 mg) were heated from 25 to 650 °C at a rate of 10 °C/min in a N_2 environment.

Mechanical Characterization of Microcapsules. The mechanical response of microcapsules was investigated using single capsule compression apparatus as described by Keller and Sottos.[44] Displacement was applied at a rate of 1 μm/s using a stepper actuator (Physik Insturmente M-230S) attached to the testing apparatus and was controlled via computer interface. Load data were acquired from a 10 g load cell (Transducer Techniques GSO-10) via a DAQ card (PCI-MIO-16E-4) and associated software from National Instruments giving a combined sensor system accuracy of ±100 nN. Images of the capsule during the compression cycle were captured through a stereo microscope (Nikon SMZ-2T) by a monochrome CCD camera (QImaging Retiga). The entire system was mounted on a vibration isolation table.

Before testing, microcapsules were drawn into a pipet, which enabled release of a single capsule onto the compression platen. An image of the microcapsule was taken prior to compression to determine the initial capsule diameter. An initial separation between the capsule and punch allowed the stepper to achieve steady-state velocity after motion was initiated. The test program was started after positioning the punch above the capsule, and terminated after failure was observed.

3. Results and Discussion

3.1. Selection of Prepolymer. A number of commercial PU prepolymers (Air Products: Airthane PHP-80D, BayerMaterial: Desmodur E-14, E-1361) were evaluated as potential microcapsule shell wall precursors, but all failed to produce high-quality microcapsules. However, encapsulations using the synthesized PU prepolymer[31] were successful. The average NCO content of the successful prepolymer is 20.1 ± 0.6 wt % as determined by titration. This content is higher than that of the commercial prepolymers, which ranged from 3 to 11%. The higher NCO content in the prepolymer was essential for robust shell wall formation.

3.2. Processing and Characterization of Microcapsules. Diisocyanate-filled microcapsules were prepared by interfacial polymerization in an oil and water emulsion. The PU prepolymer was dissolved in chlorobenzene. A water-soluble diol served as a chain extender for the capsule shell wall, since the relative rate of reaction of the diol/NCO is 1 order of magnitude higher than that of water/NCO.[45] Additionally, the diol might favorably diffuse into the organic phase and promote surface reactions prior to significant hydrolysis of isocyanate with water. The large difference in reactivities of IPDI and TDI[45] led to stable shell wall formation and capsules with a high IPDI fill content.

Table 1. Geometric Parameters of the Microcapsules Synthesized at Different Agitation Rates

agitation rate (rpm)	500	700	900	1100	1500
D, diameter (μm)[a]	413 ± 124	205 ± 73	103 ± 34	67 ± 17	39 ± 9
h, wall thickness (μm)[a]	17 ± 4	10 ± 2	4 ± 2	3 ± 1	2 ± 0.5
h/D	0.04	0.05	0.04	0.05	0.05

[a] Average value ±1 standard deviation.

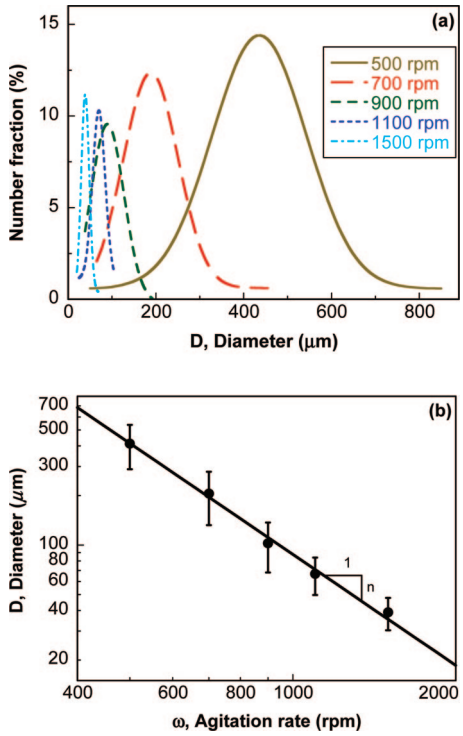

Figure 3. (a) Microcapsule size histograms at different agitation rates. (b) Average microcapsule diameter as a function of agitation rate ($n = -2.24$).

Core Materials in Microcapsules. Viability of the encapsulated IPDI was initially assessed by a simple reactivity test. A small amount of capsules was crushed between two microscope slides immediately following filtration and drying. After crushing, ethylenediamine was added to the released microcapsule contents. The released liquid rapidly gelled and produced heat, indicating that IPDI had been encapsulated and was still chemically active. The ability of the core material to polymerize in the presence of water was similarly assessed. Core material released from crushed capsules was hydrated, and after 48 h, a solid polymer layer was observed, indicating potential for healing in a water environment.

Microcapsule Size Distribution. The size of microcapsules is influenced by several factors including the geometry of the mixing device, blade hydrodynamics, viscosity, and interfacial tension of the media, shear/agitation rate, temperature, and surfactant effects. The microcapsule size distributions were measured for a range of agitation rates (500−1500 rpm) while holding all other factors constant (Table 1). From the results presented in Figure 3, the effect of increasing the agitation rate is 2-fold. With increasing agitation rate, the average diameter of the capsules decreases and the size distribution narrows. This result was also reported for urea−formaldehyde capsules of dicyclopentadiene (DCPD).[46]

Agitation rate controls the equilibrium between shear forces and interfacial tension of the discrete oil droplets and the local velocity gradient the droplets experience.[47] At low agitation rate, interfacial tension dominates and dispersed droplets remain large. Large droplets are broken up into small ones when strong shear forces are experienced under high agitation rate. In addition, the average diameter exhibits a power-law relationship ($n = -2.24$) with agitation rate, as shown in Figure 3b. Accordingly, the processing conditions for optimal capsule size can be determined for high healing efficiency according to the size of expected damage.[48]

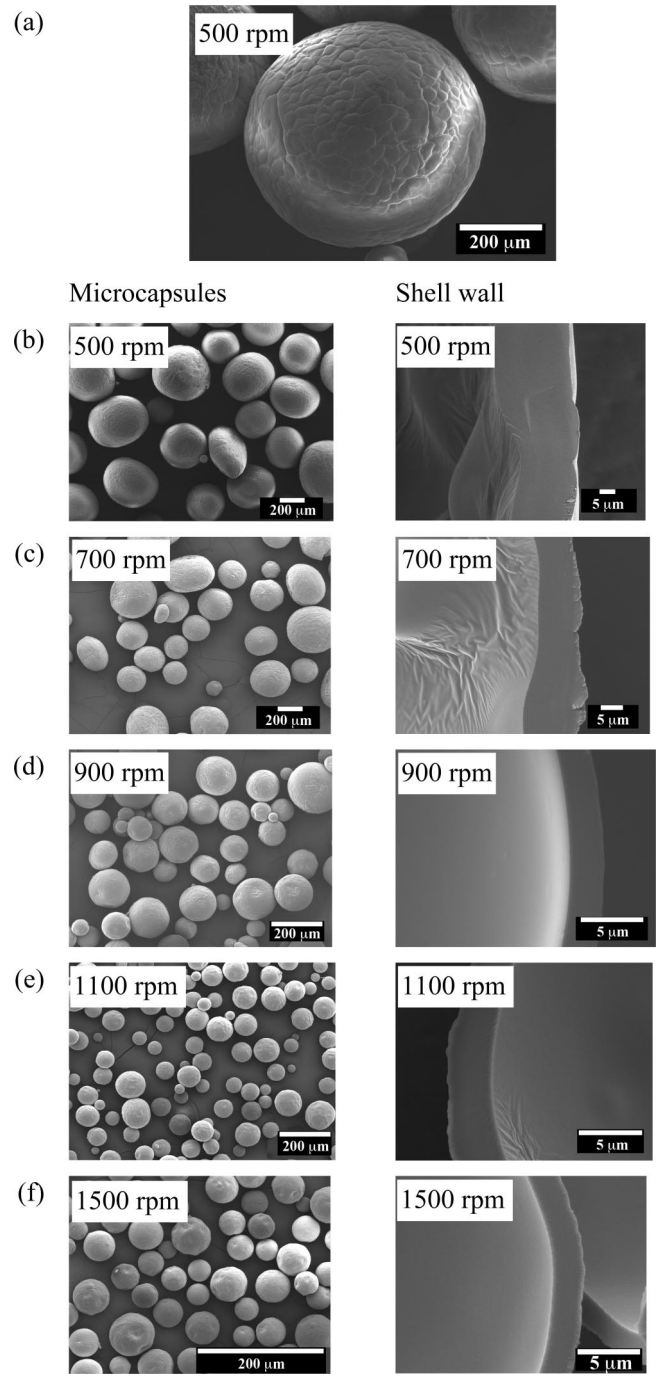

Figure 4. Surface and shell morphology of microcapsules obtained at various agitation rates.

Surface Morphology. The surface and shell morphology of microcapsules synthesized under various agitation rates was observed using SEM and are presented in Figure 4. Spherical microcapsules are obtained at all agitation rates although a few elongated (ellipsoidal) shapes appear at low agitation rates (Figure 4b). For all cases, the outer surface of the capsules is relatively smooth with some wrinkling resulting from the interaction of inhomogeneous reaction kinetics, fluid-induced shear forces, and shell-determined elastic forces[49] (Figure 4a).

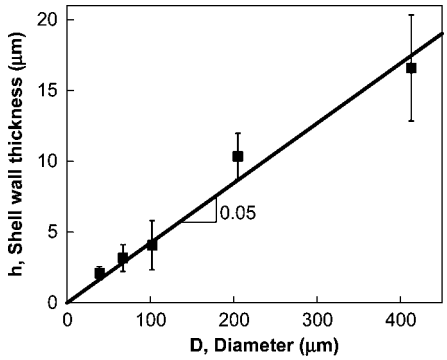

Figure 5. Average shell wall thickness as a function of microcapsule diameter.

The inner surface is generally smoother, since little shear flow occurs inside the capsule during the formation of the shell wall.

Shell Wall. The mean shell wall thickness as a function of agitation rates is plotted in Figure 5. Mean wall thickness scales linearly with capsule diameter over the range of agitation rates investigated (Table 1). The ratio of shell wall thickness to capsule diameter is relatively constant with a mean value of 0.05.

At low agitation rates (≤700 rpm), the shell wall is greater than 10 μm thick and varies significantly in a single capsule. Since the capsules are relative large under these conditions, the specific interface area is reduced and more polymerized product is formed at interface. Because of locally inhomogeneous reaction kinetics and diffusion of diol molecules, a nonuniform and thick shell wall is produced. At higher shear rates (≥900 rpm), the shell wall is more uniform and much smaller since the interfacial area is increased and a more homogeneous reaction occurs.

Thermal Properties and Components Analysis. The thermal properties of filled microcapsules as well as pure ClB, IPDI, and shell wall material (obtained from crushed capsules) are characterized by thermogravimetric analysis (TGA). The resultant curves of mass loss for each material are presented in Figure 6a as a function of temperature. For the neat components, ClB evaporates completely by 100 °C while IPDI begins to evaporate at 120 °C and finishes by 240 °C. The shell wall material loses about 5% of weight below 250 °C presumably from absorbed water and precipitously decomposes above 300 °C with about 20% of the original mass remaining at 600 °C. Representative rate of mass loss curves are shown in Figure 6b for 900 rpm capsules.

Microcapsules synthesized at different agitation rates all have similar thermal behavior. Release of liquid core materials (ClB and IPDI) from microcapsules occurs at a higher temperature when compared with the unencapsulated components. For all capsules, there is less than 3% mass loss before 110 °C, indicating only a small amount of adsorbed water on the microcapsule surface. The mass loss at 120 °C correlates to the onset of diffusion of ClB contained within the microcapsule. Mass loss peaks at 250 °C are indicative of the evaporation of the IPDI (see Supporting Information, Figures S1 and S2). The final mass loss peaks are associated with the decomposition of the shell wall, which overlap for all microcapsule batches, indicating there is no remaining ClB or IPDI above 280 °C, as shown in Figure 6b.

The weight percentage of each component in the microcapsules is estimated based on analysis of the TGA data and calculation of the mass loss rates. As shown in Figure 7, the contents of core and shell materials are 68 and 32 wt %, respectively, for all batches of microcapsules. The content of IPDI in the core is 63 wt % at agitation rates below 900 rpm,

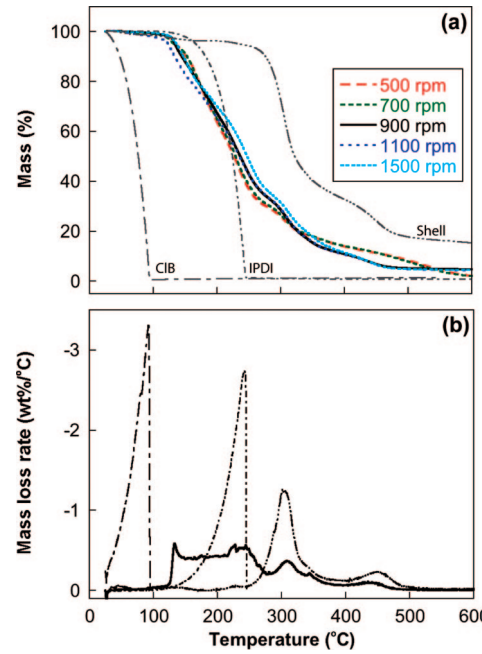

Figure 6. (a) TGA weight loss curves of synthesized microcapsules along with authentic traces for ClB, IPDI, and shell wall material. (b) Derivatives of TGA data of ClB, IPDI, shell, and 900 rpm capsules. All experiments were conducted at a heating rate of 10 °C/min in a N_2 environment.

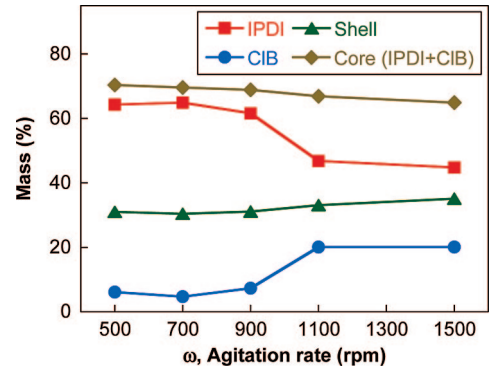

Figure 7. Evaluation of component weight fractions of microcapsules via TGA data analysis.

but decreases to 45 wt % at the agitation rates above 1100 rpm. Correspondingly, the percentage of ClB in the core is as low as 6 wt % at intermediate and low agitation rates but increases to 20 wt % at high agitation rates.

Shelf Life. The shelf life of IPDI filled microcapsules produced at 900 rpm was investigated by TGA experiments. Capsules were stored in a sealed glass vial at room temperature for 3.5 and 6 months and then analyzed by TGA to observe the component change (Figure 8a). A reduction of IPDI core material of 7.9 and 8.6 wt % was obtained after 3 and 6 months storage at ambient temperature, respectively. This reduction in IPDI core content is equivalent to the subsequent increase in shell wall material (Figure 8b), indicating that some IPDI is slowly reacting with diffused water to form new shell wall material. Additionally, encapsulated IPDI released from the fractured capsules between two glass slides continues to show good reactivity upon contact with amines, bonding the slides tightly.

Mechanical Properties. Individual microcapsules were tested in diametral compression to determine the elastic stiffness of the shell wall and the strength of the microcapsule following the method of Keller and Sottos.[44] Representative compression

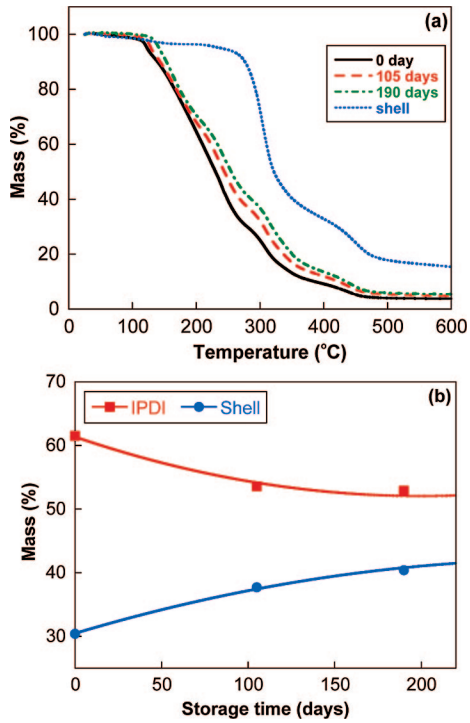

Figure 8. (a) TGA weight loss curves of microcapsules (900 rpm) after 105 and 180 days storage at room temperature in comparison with the fresh capsules and shell wall material. (b) Component weight fractions as a function of storage time.

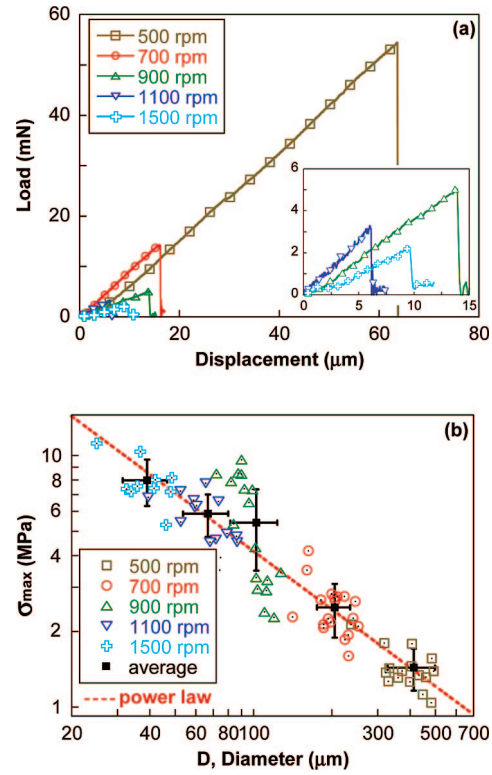

Figure 9. (a) Representative compression loading curves of microcapsules. (b) Normalized maximum strength as a function of capsules size along with power law fit to data ($n = -0.77$). Solid symbols represent the average values along with the standard deviation of different batches of capsules.

loading curves for a variety of microcapsule diameters are shown in Figure 9a. For all batches of capsules, the load increases linearly with applied displacement until reaching a maximum value. Larger capsules sustain higher loads before rupture due to their thicker shell walls. Video recording of the compression tests confirm that the microcapsule failure coincides with the maximum load. After failure, the encapsulated fluid leaks out of the microcapsules.

The normalized maximum strength, σ_{max}, is calculated from

$$\sigma_{max} = \frac{4P_{max}}{\pi(D_o - D_i)^2} \quad (2)$$

where P_{max} is the maximum load and D_o and D_i are the outer and inner diameter of the capsules, respectively. The average value of σ_{max} is plotted in Figure 9b as a function of microcapsule diameter and scales as a power law with deceasing microcapsule size. The strength data indicate that smaller capsules are much stronger than their larger counterparts, which is in agreement with the conclusion of Keller and Sottos for a urea−formaldehyde microcapsule system.[35]

4. Conclusion

Liquid IPDI-filled microcapsules were successfully synthesized by interfacial polymerization of a TDI-derived polyurethane prepolymer in an oil-in-water emulsion. Spherical microcapsules with average diameter in the range of 40−400 μm were manufactured by adjusting agitation rate over the range of 500−1500 rpm. The mean diameter and agitation rate followed an inverse power law relationship. Once the microcapsules were filtered and dried, free-flowing powder was obtained with high yields. The average shell wall thickness ranged from 2 to 17 μm and increased linearly with capsule diameter, yielding a nearly constant wall thickness to diameter ratio of 0.05. IPDI content in capsules was above 60 wt % at agitation rates below 900 rpm, and weight loss was less than 10 wt % after half-year storage. Capsules were linear elastic in compression to failure and the average strength decreases with increasing diameter.

IPDI-filled capsules will enable new healing chemistries for self-healing polymers that are robust and stable and are single-component catalyst-free systems. Their performance in self-healing coatings is currently under evaluation.

Acknowledgment. The authors acknowledge Bayer MaterialScience and AFOSR (Grants FA9550-06-1-0553 and FA 9550-05-1-0346) for the support of this research. Electron microscopy was performed in the Imaging Technology Group, Beckman Institute at the University of Illinois at Urbana−Champaign. Special thanks are given to Karl Haider and Brent Crenshaw from Bayer MaterialScience for valuable discussions on isocyanates and providing raw materials.

Supporting Information Available: Synthesis of the urethane prepolymer, DSC of shell wall from crushed microcapsules, and SEM images of microcapsules baked at higher temperature. This material is available free of charge via the Internet at http://pubs.acs.org.

References and Notes

(1) van der Zwaag, S. *Self Healing Materials: An Alternative Approach to 20 Centuries of Materials Science*; Springer: New York, 2007.
(2) Kessler, M. R. *Proc. I MECH E Part G J. Aerospace Eng.* **2007**, *221*, 479–495.
(3) Youngblood, J. P.; Sottos, N. R. *MRS Bull.* **2008**, *33*, 732–741.
(4) White, S. R.; Caruso, M. M.; Moore, J. S. *MRS Bull.* **2008**, *33*, 766–769.
(5) Wu, D. Y.; Meure, S.; Solomon, D. *Prog. Polym. Sci.* **2008**, *33*, 479–522.
(6) White, S. R.; Sottos, N. R.; Geubelle, P. H.; Moore, J. S.; Kessler,

M. R.; Sriram, S. R.; Brown, E. N.; Viswanathan, S. *Nature (London)* **2001**, *409*, 794–797.
(7) Caruso, M. M.; Delafuente, D. A.; Ho, V.; Sottos, N. R.; Moore, J. S.; White, S. R. *Macromolecules* **2007**, *40*, 8830–8832.
(8) Kamphaus, J. M.; Rule, J. D.; Moore, J. S.; Sottos, N. R.; White, S. R. *J. R. Soc.: Interface* **2008**, *5*, 95–103.
(9) Yuan, L.; Gu, A.; Liang, G. *Mater. Chem. Phys.* **2008**, *110*, 417–425.
(10) Yin, T.; Rong, M. Z.; Zhang, M. Q.; Yang, G. C. *Compos. Sci. Technol.* **2007**, *67*, 201–212.
(11) Cosco, S.; Ambrogi, V.; Musto, P.; Carfagna, C. *J. Appl. Polym. Sci.* **2007**, *105*, 1400–1411.
(12) Jones, A. S.; Rule, J. D.; Moore, J. S.; White, S. R.; Sottos, N. R. *Chem. Mater.* **2006**, *18*, 1312–1317.
(13) Rule, J. D.; Brown, E. N.; Sottos, N. R.; White, S. R.; Moore, J. S. *Adv. Mater.* **2005**, *17*, 205–208.
(14) Brown, E. N.; White, S. R.; Sottos, N. R. *Compos. Sci. Technol.* **2005**, *65*, 2466–2473.
(15) Brown, E. N.; White, S. R.; Sottos, N. R. *Compos. Sci. Technol.* **2005**, *65*, 2474–2480.
(16) Kessler, M. R.; Sottos, N. R.; White, S. R. *Composites, Part A* **2003**, *34*, 743–753.
(17) Brown, E. N.; Sottos, N. R.; White, S. R. *Exp. Mech.* **2002**, *42*, 372–379.
(18) Yuan, Y. C.; Rong, M. Z.; Zhang, M. Q.; Chen, J.; Yang, G. C.; Li, X. M. *Macromolecules* **2008**, in press.
(19) Williams, H. R.; Trask, R. S.; Bond, I. P. *Smart Mater. Struct.* **2007**, *16*, 1198–1207.
(20) Williams, G.; Trask, R.; Bond, I. *Composites, Part A* **2007**, *38*, 1525–1532.
(21) Trask, R. S.; Williams, G. J.; Bond, I. P. *J. R. Soc.: Interface* **2007**, *4*, 363–371.
(22) Trask, R. S.; Bond, I. P. *Smart Mater. Struct.* **2006**, *15*, 704–710.
(23) Pang, J. W. C.; Bond, I. P. *Compos. Sci. Technol.* **2005**, *65*, 1791–1799.
(24) Toohey, K. S.; Sottos, N. R.; Lewis, J. A.; Moore, J. S.; White, S. R. *Nat. Mater.* **2007**, *6*, 581–585.
(25) Williams, H. R.; Trask, R. S.; Knights, A. C.; Williams, E. R.; Bond, I. P. *J. R. Soc.: Interface* **2008**, *24*, 735–747.
(26) Bejan, A.; Lorente, S.; Wang, K. M. *J. Appl. Phys.* **2006**, *100*, Article #: 033528.
(27) Bergman, S. D.; Wudl, F. *J. Mater. Chem.* **2008**, *18*, 41–62.
(28) Bergman, S. D.; Wudl, F. Remendable polymers. In *Self Healing Materials*; Zwaag, S. v. d., Ed.; Springer: New York, 2007; pp 45−68.
(29) Chen, X. X.; Wudl, F.; Mal, A. K.; Shen, H. B.; Nutt, S. R. *Macromolecules* **2003**, *36*, 1802–1807.
(30) Chen, X. X.; Dam, M. A.; Ono, K.; Mal, A.; Shen, H. B.; Nutt, S. R.; Sheran, K.; Wudl, F. *Science* **2002**, *295*, 1698–1702.
(31) Cho, S. H. Polydimethylsiloxane-based self-healing composite and coating materials. PhD Thesis, University of Illinois at Urbana−Champaign, Urbana, **2007**.
(32) Shchukin, D. G.; Mohwald, H. *Small* **2007**, *3*, 926–943.
(33) Feng, W.; Patel, S. H.; Young, M. Y.; Zunino, J. L.; Xanthos, M. *Adv. Polym. Technol.* **2007**, *26*, 1–13.
(34) Kumar, A.; Stephenson, L. D.; Murray, J. N. *Prog. Org. Coat.* **2006**, *55*, 244–253.
(35) Zheludkevich, M. L.; Shchukin, D. G.; Yasakau, K. A.; Mohwald, H.; Ferreira, M. G. S. *Chem. Mater.* **2007**, *19*, 402–411.
(36) Lamaka, S. V.; Zheludkevich, M. L.; Yasakau, K. A.; Serra, R.; Poznyak, S. K.; Ferreira, M. G. S. *Prog. Org. Coat.* **2007**, *58*, 127–135.
(37) Ahmad, Z. *Principles of Corrosion Engineering and Corrosion Control*; Elsevier: Amsterdam, 2006.
(38) Cho, S. H.; Andersson, H. M.; White, S. R.; Sottos, N. R.; Braun, P. V. *Adv. Mater.* **2006**, *18*, 997–1000.
(39) Yang, H.; Mendon, S. K.; Rawlins, J. W. In 233rd ACS National Meeting, American Chemical Society, Chicago, **2007**.
(40) Cheong, I. W.; Kim, J. H. *Chem. Commun.* **2004**, 2484–2485.
(41) Querat, E.; Tighzert, L.; Pascault, J. P. *J. Coat. Technol.* **1996**, *68*, 83–90.
(42) Randall, D.; Lee, S. *The Polyurethanes Book*; John Wiley & Sons: New York, 2002.
(43) Ye, A.; Flanagan, J.; Singh, H. *Biopolymers* **2006**, *82*, 121–133.
(44) Keller, M. W.; Sottos, N. R. *Exp. Mech.* **2006**, *46*, 725–733.
(45) Shaffer, M. W. ICE 2004 Technology Conference, Chicago, Oct 25−29, **2004**.
(46) Brown, E. N.; Kessler, M. R.; Sottos, N. R.; White, S. R. *J. Microencapsulation* **2003**, *20*, 719–730.
(47) Rallison, J. M. *Annu. Rev. Fluid Mech.* **1984**, *16*, 45–66.
(48) Rule, J. D.; Sottos, N. R.; White, S. R. *Polymer* **2007**, *48*, 3520–3529.
(49) Finken, R.; Seifert, U. *J. Phys.: Condens. Matter* **2006**, *18*, L185−L191.

MA801718V